Acta Alimentaria 50 (2021) 2, 199–209
DOI: 10.1556/066.2020.00225

AKADÉMIAI KIADÓ

Modelling and optimisation of chitosan anchored titanium dioxide nano-adsorbent for dairy industry effluent treatment

B.L. Dinesha[1*], S. Hiregoudar[1], U. Nidoni[2], K.T. Ramappa[2], A.T. Dandekar[3] and M.V. Ravi[4]

[1] Centre for Nanotechnology, College of Agricultural Engineering, University of Agricultural Sciences, Raichur, Karnataka, India

[2] Department of Processing and Food Engineering, College of Agricultural Engineering, University of Agricultural Sciences, Raichur, Karnataka, India

[3] College of Agriculture, Mandya, University of Agricultural Sciences, Bangalore, Karnataka, India

[4] Department of Soil Science and Agricultural Chemistry, College of Agriculture, University of Agricultural Sciences, Raichur, Karnataka, India

ORIGINAL RESEARCH PAPER

Received: August 09, 2020 • Accepted: January 29, 2021
Published online: March 15, 2021

Check for updates

ABSTRACT

The present study emphasised the efficiency of chitosan anchored titanium dioxide nano-adsorbent on dairy industry effluent treatment. Chitosan titanium dioxide nano-adsorbent was synthesised by using chemical precipitation method and characterised for its particle size, surface morphology and texture. A four-factor-three-level Box–Behnken design along with response surface methodology was used to optimise the adsorption process parameters. Linear, two factor interaction, quadratic and cubic model techniques were used to demonstrate the influence of each parameter and their interaction effects on the responses. The quadratic models derived from the experimental data were used to predict the maximum per cent reduction of biological oxygen demand (BOD) and chemical oxygen demand (COD). The optimised treatment combination for maximum per cent reduction in BOD (90.48%) and COD (82.10%)

* Corresponding author. E-mail: dinirbdgtc@gmail.com

was found to be initial concentration of 100 mg L^{-1}, pH of 7, dosage of 1.25 mg L^{-1} and contact time of 100 min.

KEYWORDS

chitosan titanium dioxide, nano-adsorbent, dairy industry, effluent, modelling

1. INTRODUCTION

Industrialisation is an important tool for the development of any nation. Consequently, the industrial activities has expanded so much all over the world today, that it has become a matter of concern due to the deteriorating environment (Farizoglu and Uzuner, 2011). With the rapid growth of industries in India, pollution of natural water by individual venture has increased tremendously (Hu et al., 2006). Dairy industry (DI) is one of the major food industries responsible for water pollution. In India, DI has been reported to emit huge amounts of wastewater (approximately 2–20 L) per litre of processed milk (Thirugnanasambandham and Ganesamoorthy, 2019).

DI wastewater is generated through the operation of various milk and milk based products processing units at cleaning, washing, cooling, heating. etc. DI wastewater contains milk constituents such as whey protein, lactose, fat and minerals in high concentrations (Farizoglu and Uzuner, 2011). These constituents are malodorous due to their susceptibility to oxidation and decomposition processes (Sarkar et al., 2006). According to previous studies, conventional wastewater treatment technologies have several disadvantages, such as huge investment costs and low treatment efficiency (Thirugnanasambandham et al., 2014a).

Recently, membrane technology in DI wastewater treatment has been researched by many (Thirugnanasambandham and Shine, 2016a). Major disadvantage of membrane based technologies is fouling; hence requiring regular maintenance (Farizoglu and Uzuner, 2011). Application of nanotechnology through the usage of nano-adsorbents for the treatment of industrial wastewater could be one of the most promising technologies with a considerable potential (Thirugnanasambandham and Sivakumar, 2015). Nano-adsorbents have large active surface area, high adsorption capacity and are hydrophilic in nature. Hence, several oxide based nano-adsorbents, such as zinc oxide, titanium dioxide, nickel oxide, copper oxide, iron oxide and graphene oxide, could be used effectively (El-Sayed, 2020).

There are no scientific reports published on the application of chitosan titanium dioxide ($CTiO_2$) nano-adsorbent for removal of organic pollutants from DI wastewater. Hence, the present investigation focused on synthesising and characterising $CTiO_2$ nano-adsorbent for effective treatment of DI wastewater. The outcome of this study would offer a solution for the dairy industry with an economical and efficient way to treat dairy wastewater.

2. MATERIALS AND METHODS

2.1. Synthesis and characterisation of $CTiO_2$

$CTiO_2$ nano-adsorbent was synthesised according to the method described by Alagumuthu and Kumar (2013) and characterised by using particle size analyser, scanning electron microscope with elemental detection sensor (SEM-EDS) and atomic force microscope (AFM).

2.2. Batch adsorption study

Batch adsorption study was conducted for per cent reduction in BOD and COD of model solution by using $CTiO_2$ nano-adsorbent by following the method described by Thirugnanasambandham et al. (2014a). Synthetic BOD solution was prepared by dissolving 150 mg L^{-1} of glucose in glutamic acid (i.e. 1,000 mg L^{-1} stock solution). Synthetic COD solution was prepared by dissolving 0.085 g of potassium hydrogen phthalate in 1 L distilled water (i.e. 1,000 mg L^{-1} stock solution).

The model solution was treated with three dosages of $CTiO_2$ (0.50, 1.25 and 2.00 mg L^{-1}) at three different BOD and COD concentrations (100, 200 and 300 mg L^{-1}) at three different pH levels (2, 7 and 12) for three contact times (20, 60 and 100 min). The per cent reduction in BOD and COD of the model solution was calculated by using Eq. (1),

$$\%\,\text{reduction} = \left[\frac{C_0 - C_e}{C_0}\right] \times 100 \quad (1)$$

where, C_o and C_e: Initial and final BOD and COD concentrations of model solution (Thirugnanasambandham et al., 2014b).

2.3. Statistical experimental design

Statistical analysis of experimental results was carried out by using 'design expert' software (8.0.7.1 version). Three levels-four factors response surface methodology (RSM) with Box-Behnken design (BBD) was adopted to study the individual and interaction effects of selected variables (Liu and Peng, 2017). The independent variables with their levels are listed in Table 1. There were twenty-nine experiments designed with five centre points and replicated thrice.

3. RESULTS AND DISCUSSION

3.1. Characterisation of synthesised $CTiO_2$ nano-adsorbent

The synthesised $CTiO_2$ nano-adsorbent was found to have average particle size of 87.43 d.nm. Sharp peaks obtained in the particles were of similar size and uniformly distributed throughout the mass (Fig. 1). Synthesised $CTiO_2$ nano-adsorbent particle structures were rod shaped or

Table 1. Independent variables and their levels for per cent reduction in BOD and COD of model solution by using $CTiO_2$ nano-adsorbent

Variables	Unit	Factors	Levels		
			Low (−1)	Middle (0)	High (+1)
Initial concentration of model BOD and COD solutions	mg L^{-1}	X_1	100	200	300
pH of model BOD and COD solutions		X_2	2	7	12
Dosage of $CTiO_2$	mg L^{-1}	X_3	0.50	1.25	2.00
Contact time of $CTiO_2$	Min	X_4	20	60	100

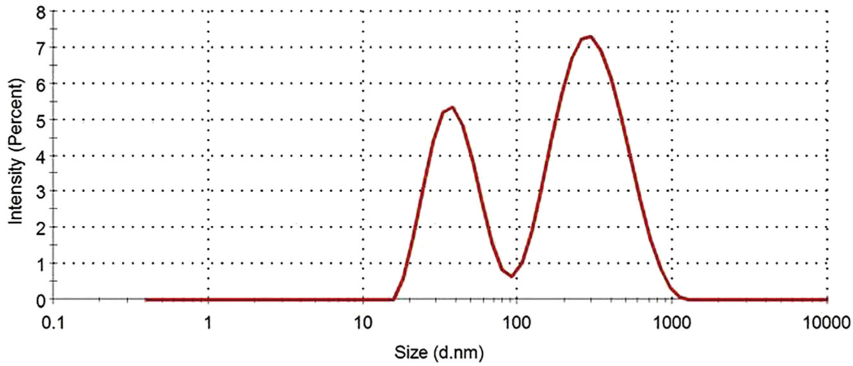

Fig. 1. Average particle size of synthesised $CTiO_2$ nano-adsorbent

aggregated with rough surface (Fig. 2A). The desired rough surface formation of the aggregates was achieved with higher sodium hydroxide concentration during synthesis (Kavitha et al., 2013).

EDS spectra showed a major amount of titanium (68.30%) followed by chitosan (30.56%) and negligible amount of sodium (1.14%) (Fig. 2B). Sodium traces in the composite material are due to sintering of residual sodium during the synthesis process (Raut et al., 2016). Average height and surface roughness of $CTiO_2$ nano-adsorbent were 65.49 nm and 0.99 nm, respectively (Fig. 3A and 3B). Higher roughness was achieved due to the agglomeration of $CTiO_2$ composite (Tian et al., 2003). Topography and profile images of AFM revealed an expected rough surface texture consisting of particles fused together at inter-particle contact points (Hu et al., 2006).

3.2. Effect of process variables on per cent reduction of BOD and COD

The values of per cent reduction in BOD and COD of model solution for different independent variables are presented in Table 2. The interaction effects are discussed hereunder.

The effect of pH and initial BOD and COD concentrations on per cent reduction of BOD and COD is depicted in Fig. 4A. Per cent reduction of BOD and COD increased with the

A B

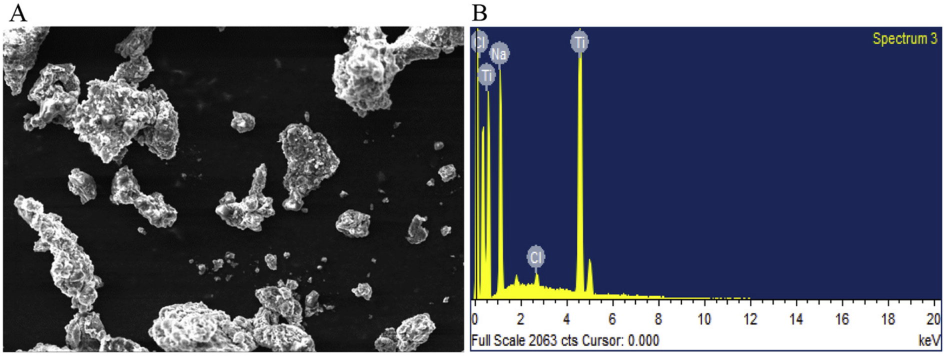

Fig. 2. SEM image (A) and EDS spectrum (B) of $CTiO_2$ nano-adsorbent

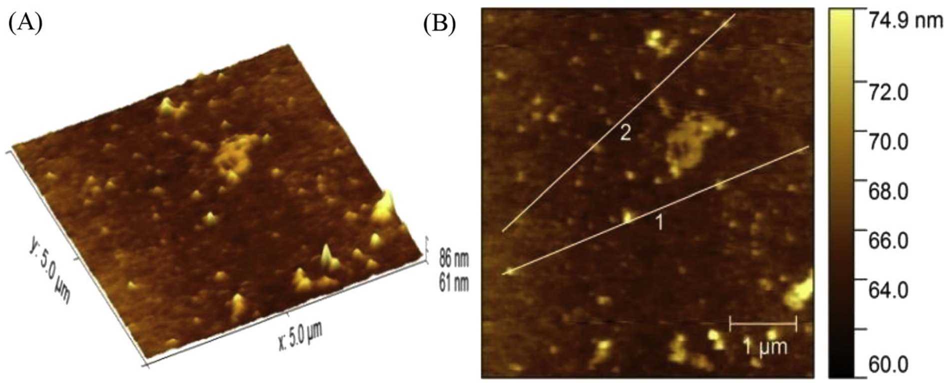

Fig. 3. Topography (A) and profile (B) images of $CTiO_2$ nano-adsorbent obtained by AFM

increase in the pH of the solution from 2 to 12. This might be due to the conversion of hydroperoxyl radicals (HOO•) and hydroxyl radicals (OH•) into hydrogen peroxide at lower pH (Akthar et al., 2007). On the other hand, as the initial concentration of BOD and COD increased from 100 to 300 mg L^{-1}, the per cent reduction of BOD and COD in model solution decreased. This was due to hydroxyl radical scavenging activity. SO_4^{2-}, NO_3^-, CO_3^{2-} and Cl^- ions might have blocked the active sites on the $CTiO_2$ surface (Bhanarkar et al., 2014). The effect of $CTiO_2$ dosage and initial BOD and COD concentrations on per cent reduction of BOD and COD in the model solution is illustrated in Fig. 4B. It can be seen that as the dosage of $CTiO_2$ increased from 0.5 to 2.00 mg L^{-1}, the per cent reduction of BOD and COD in model solution increased as well. It is presumed that the availability of active sites on the $CTiO_2$ nano-adsorbent considerably increased at higher doses (Thirugnanasambandham et al., 2014a). On the other hand, as the initial concentration increased from 100 to 300 mg L^{-1}, the per cent reduction of BOD and COD decreased. A possible explanation is that the higher initial concentration resulted in more adsorption of organic substances on the surface of the adsorbent (Farzana and Meenakshi, 2013). When the contact time with nano-adsorbent particles in model effluent solution increased from 20 to 100 min, the per cent reduction of BOD and COD also increased (Fig. 4C). This might be due to the nature of organic pollutants, which require longer time for adsorption (Karthikeyan et al., 2017).

3.3. Box-Behnken design

Different levels of input variables were set to observe their effect on per cent reduction of BOD and COD in model solution by using $CTiO_2$ nano-adsorbent. The interaction relationship of variables was determined by fitting the quadratic equation to the obtained data (Reddy et al., 2014). For four factors ($n = 4$) and three levels (low (–), medium (0) and high (+)) the fitted quadratic response model is given in Eq. (2).

$$Y = b_1X_1 + b_2X_2 + b_3X_3 + b_4X_4 + b_{11}X_{12} + b_{22}X_{22} + b_{33}X_{32} + b_{44}X_{42} + b_{12}X_1X_2 + b_{13}X_1X_3 + b_{14}X_1X_4 + e, \quad (2)$$

Table 2. Coded and un-coded Box-Behnken design of independent variables and their corresponding experimental values

					Per cent reduction			
					BOD		COD	
Run	X_1 (mg L^{-1})	X_2	X_3 (mg L^{-1})	X_4 (min)	Exp.	Pred.	Exp.	Pred.
1	100(−1)	2(−1)	1.25(0)	60(0)	88.56	88.41	82.10	82.02
2	300(+1)	2(−1)	1.25(0)	60(0)	25.59	25.51	62.27	62.11
3	100(−1)	12(+1)	1.25(0)	60(0)	86.42	86.40	80.15	80.02
4	300(+1)	12(+1)	1.25(0)	60(0)	23.04	23.11	50.17	50.57
5	200(0)	7(0)	0.5(−1)	20(−1)	50.41	50.30	41.12	41.28
6	200(0)	7(0)	2(+1)	20(−1)	56.84	56.54	46.98	46.71
7	200(0)	7(0)	0.5(−1)	100(+1)	52.45	52.56	44.52	44.67
8	200(0)	7(0)	2(+1)	100(+1)	55.18	55.28	51.48	51.65
9	100(−1)	7(0)	1.25(0)	20(−1)	70.50	70.35	78.05	77.84
10	300(+1)	7(0)	1.25(0)	20(−1)	20.81	22.40	45.63	45.41
11	100(−1)	7(0)	1.25(0)	100(+1)	90.48	89.07	81.21	81.01
12	300(+1)	7(0)	1.25(0)	100(+1)	28.77	28.25	55.31	55.58
13	200(0)	2(−1)	0.5(−1)	60(0)	51.25	51.06	35.05	35.29
14	200(0)	12(+1)	0.5(−1)	60(0)	51.05	51.20	33.50	33.91
15	200(0)	2(−1)	2(+1)	60(0)	66.18	66.47	36.12	36.37
16	200(0)	12(+1)	2(+1)	60(0)	65.85	64.46	38.86	38.47
17	100(−1)	7(0)	0.5(−1)	60(0)	87.16	87.22	78.95	78.54
18	300(+1)	7(0)	0.5(−1)	60(0)	24.64	24.48	48.29	48.56
19	100(−1)	7(0)	2(+1)	60(0)	87.26	87.06	71.54	71.19
20	300(+1)	7(0)	2(+1)	60(0)	27.95	27.51	46.52	46.27
21	200(0)	2(−1)	1.25(0)	20(−1)	55.62	55.46	40.68	40.97
22	200(0)	12(+1)	1.25(0)	20(−1)	54.06	54.87	34.41	34.54
23	200(0)	2(−1)	1.25(0)	100(+1)	59.42	59.09	44.30	44.18
24	200(0)	12(+1)	1.25(0)	100(+1)	57.49	57.69	41.25	41.12
25	200(0)	7(0)	1.25(0)	60(0)	58.00	58.12	39.56	39.28
26	200(0)	7(0)	1.25(0)	60(0)	58.15	57.65	39.51	39.70
27	200(0)	7(0)	1.25(0)	60(0)	58.2	58.87	39.51	39.11
28	200(0)	7(0)	1.25(0)	60(0)	58.12	58.04	39.54	39.95
29	200(0)	7(0)	1.25(0)	60(0)	58.10	58.37	39.55	39.37

X_1: Initial concentration of model BOD and COD solutions; X_2: pH of model BOD and COD solutions; X_3: Dosage of $CTiO_2$; and X_4: Contact time of $CTiO_2$.

where, Y is the predicted value of response (per cent reduction in BOD and COD); b_1, b_2, b_3 and b_4 are the linear coefficients; b_{11}, b_{22}, b_{33} and b_{44} are the quadratic coefficients; b_{12}, b_{13} and b_{14} are the cross-products coefficients; and e is the error term.

3.4. Development of a mathematical model

Different response functions such as linear, interactive, quadratic and cubic were employed to compare the experimental data (Thirugnanasambandham and Sivakumar, 2015). Two tests such as model sequential sum of squares and summary statistics of model were used to check the test

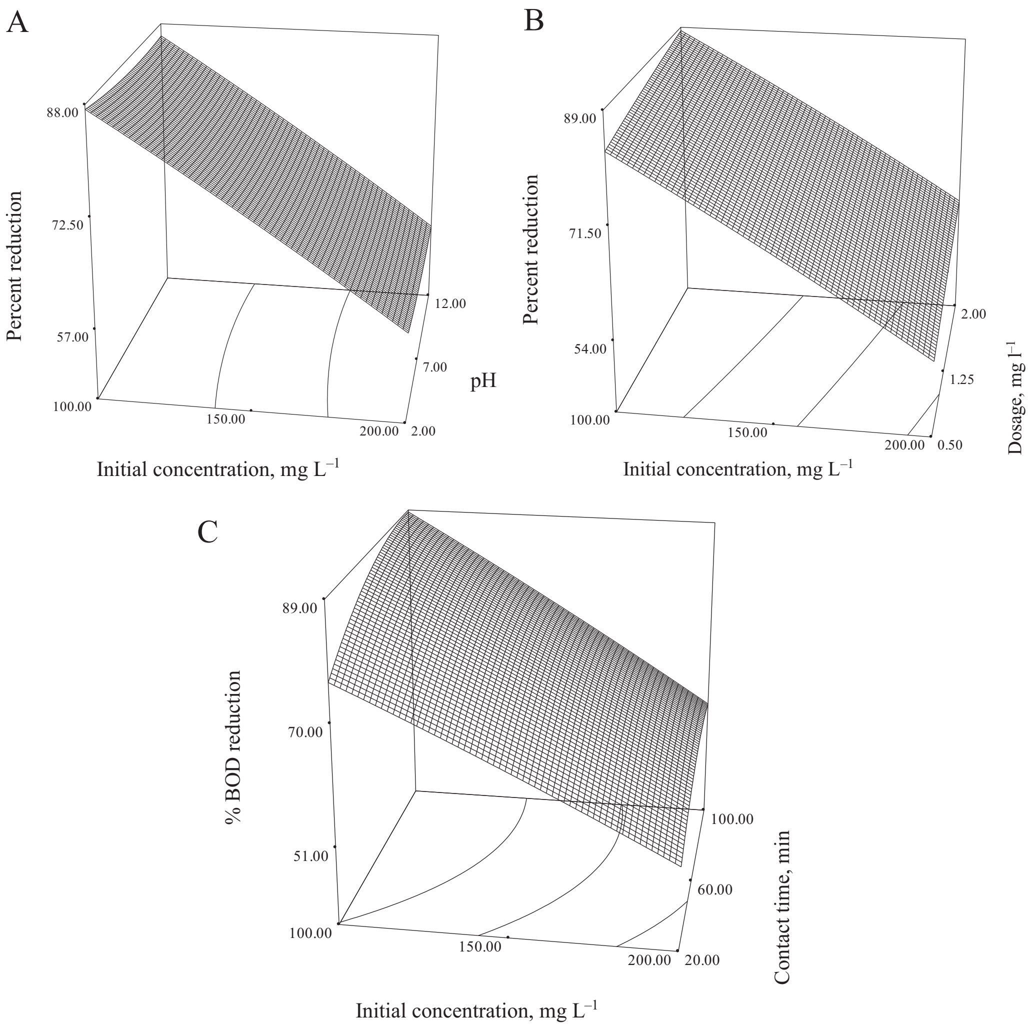

Fig. 4. Response surface plots for per cent reduction in BOD and COD in model solution using $CTiO_2$ nano-adsorbent as a function of (A) pH, (B) $CTiO_2$ dosage and (C) contact time

of significance by using BBD (Table 3). The experimental data was fitted with linear, two factor interaction (2FI), quadratic and cubic models. All these models were statistically significant as p-value lower than 0.0001. Among the tested models, quadratic model resulted the lowest values of standard error deviation (SD = 1.54), coefficient of variance (C.V = 2.74) and per cent root error sum of squares (PRESS = 603.06) for per cent reduction of BOD and COD. The higher value of R^2 (0.998), Adj. R^2 (0.990) and Pred. R^2 (0.947) indicated a strong correlation and dependence between the predicted and observed values. As a result, the quadratic model was able to provide a good estimate of the response within the range of variables studied. The developed quadratic mathematical model equations (Eqs. (3) and (4)) are the following:

Table 3. Model sequential sum of squares and summary of statistics of models

Models	Std. Dev.	C.V. %	PRESS	*R*-squared	Adj *R*-squared	Pred *R*-squared
Linear	4.03	7.19	1409.84	0.965	0.960	0.876
2FI	4.40	7.84	1113.67	0.969	0.952	0.902
Quadratic	1.54	2.76	603.06	0.998	0.990	0.947
Cubic	4.18	7.45	2070.85	0.978	0.976	0.818

$$\begin{aligned}\text{Per cent reduction of BOD} = {} & 58.11 - 29.97{*}X_1 - 0.73{*}X_2 + 3.53{*}X_3 + 2.96{*}X_4 - 0.10{*}X_1{*}X_2 \\ & + 0.80{*}X_1 - 3.01{*}X_1{*}X_4 - 0.033{*}X_2{*}X_3 - 0.093{*}X_2{*}X_4 \\ & - 0.93{*}X_3{*}X_4 - 2.12{*}X_1^2 + 0.80{*}X_2^2 - 0.24{*}X_3^2 - 3.26{*}X_4^2,\end{aligned} \tag{3}$$

$$\begin{aligned}\text{Per cent reduction of COD} = {} & 39.53 - 13.65{*}X_1 - 1.85{*}X_2 + 0.84{*}X_3 + 2.60{*}X_4 - 2.54{*}X_1{*}X_2 \\ & + 1.41{*}X_1{*}X_3 - 1.63{*}X_1{*}X_4 + 1.07{*}X_2{*}X_3 + 0.81{*}X_2{*}X_4 \\ & + 0.28{*}X_3{*}X_4 + 24.90{*}X_1^2 - 0.26X_2^2 - 1.00{*}X_3^2 + 3.00{*}X_4^2,\end{aligned} \tag{4}$$

where, X_1, X_2, X_3 and X_4 are initial concentration of BOD and COD, pH, $CTiO_2$ nano-adsorbent dosage and contact time, respectively.

3.5. Statistical significance of the quadratic model

Analysis of variance (ANOVA) was used to analyse the significance of the developed quadratic model by using corresponding sum of square, degrees of freedom (DF), standard error (SE), *F*-value and *P*-value (Table 4). Higher sum of square and *F*-value were found for per cent reduction of BOD (11181.00 and 45.68) and lower for per cent reduction of COD (6775.76 and 19.36). Hence, the mathematical modelling demonstrated that the developed model is highly significant. The standard error (SE) and p-value clearly confirmed the low deviation between the experimental and predicted data, and showed the reliability of the experiment (Liu and Peng, 2017).

3.6. Model validation

In order to demonstrate the predictive capability of the model, validation of model tests were carried out at optimal parameters (Thirugnanasambandham and Shine, 2016b). The goodness of fit values (R^2, Adj-R^2 and Pred-R^2) was compared with test models (Linear, 2FI, Quadratic and Cubic models). Among the test models, quadratic model provided higher R^2, Adj-R^2 and Pred-

Table 4. Statistical significance of the quadratic model

Responses	Sum of squares	DF	SE	Mean squares	*F*-value	*P*-value
Per cent reduction of BOD	11181.00	14	1.87	798.71	45.68	<0.0001
Per cent reduction of COD	6775.76	14	2.24	483.98	19.36	<0.0001

R^2 values (0.998, 0.990 and 0.947). The results achieved under optimal conditions improved slightly as compared to the initial set of experimental data (Thirugnanasambandham and Ganesamoorthy, 2019). Mean values obtained from the verification experiments for per cent reduction of BOD and COD were found to be 89.09 and 82.02% (predicted values), respectively, at initial BOD and COD concentration of 100 mg L^{-1}, pH of 7, nano-adsorbent dose of 1.25 g L^{-1} and contact time of 100 min.

3.7. Optimisation

RSM coupled BBD was employed to optimise the process parameters to treat dairy industry wastewater using $CTiO_2$ nano-adsorbent. The responses are maximised to obtain the best conditions for the adsorption process (Oladipo et al., 2017). Therefore, the desirability function approach under BBD was used as a goal by choosing values from 0.0 (unacceptable) to 1.0 (acceptable). During optimisation, all the independent variables were kept in range and responses as maximum. Both responses (BOD and COD) were found best at optimised conditions of 100 mg L^{-1} of initial BOD and COD concentrations, pH value of 7, $CTiO_2$ nano-adsorbent dose of 1.25 g L^{-1} and contact time of 100 minutes.

4. CONCLUSIONS

$CTiO_2$ nano-adsorbent was synthesised, characterised and used for dairy industry wastewater treatment for per cent reduction of BOD and COD in model solution. A second-order quadratic model was developed with a good R^2 (0.998), Adj. R^2 (0.990) and Pred. R^2 (0.947) values for per cent reduction in BOD and COD. Analysis of variance of the test results indicated significant effect of each process variable on treatment efficiency. Optimised conditions for per cent reduction in BOD (90.48%) and COD (82.10%) were found at model solution concentration of 100 mg L^{-1}, pH of 7, nano-adsorbent dose of 1.25 g L^{-1} and contact time of 100 min. Hence, the $CTiO_2$ nano-adsorbent could be used for efficient treatment of dairy industry wastewater.

ACKNOWLEDGEMENT

The authors express their heartfelt gratitude to Rastriya Krishi Vikas Yojana (RKVY) project, UAS, Raichur and DST-SYST [SP/YO/2019/1583(G)], Government of India for the financial support extended for conducting the present investigation.

REFERENCES

Akthar, M., Hasany, S.M., Bhanger, M.I., and Iqubal, S. (2007). Low cost sorbent for the removal of methyl parathion pesticide from aqueous solutions. *Chemosphere*, 66(1): 1829–1838.

Alagumuthu, G. and Kumar, A.T. (2013). Synthesis and characterization of chitosan/TiO_2 nanocomposites using liquid phase deposition technique. *International Journal of NanoScience and Nanotechnology*, 4(1): 105–111.

Bhanarkar, A.D., Gupta, R.K., Biniwale, R.B., and Tamhane, S.M. (2014). Nitric oxide absorption by hydrogen peroxide in airlift reactor: a study using response surface methodology. *International Journal of Environmental Science and Technology*, 11(6): 1537–1548.

El-Sayed, M.E.A. (2020). Nano-adsorbents for water and wastewater remediation. *Science of the Total Environment*, 739: 139903.

Farizoglu, B. and Uzuner, S. (2011): The investigation of dairy industry wastewater treatment in a biological high performance membrane system. *Biochemical Engineering Journal*, 57(15): 46–54.

Farzana, H.M. and Meenakshi, S. (2013). Removal of acid blue 158 from aqueous media by adsorption onto cross-linked chitosan beads. *Journal of Chitin and Chitosan Science*, 1(1): 50–58.

Hu, J., Chen, G. and Lo, I.M.C. (2006). Selective removal of heavy metals from industrial wastewater using maghemite nanoparticles: performance and mechanisms. *Journal of Environmental Engineering*, 132(7): 709–715.

Karthikeyan, K.T., Nithya, A., and Jothivenkatachalama, K. (2017). Photocatalytic and antimicrobial activities of chitosan-TiO_2 nanocomposite. *International Journal of Biological Macromolecules*, 104B: 1762–1773.

Kavitha, A.K., Prabhu, M., Rajendran, V., Manivasankan, P., Prabu, P., and Jayakumar, T. (2013). Optimization of nano-titania and titania-chitosan nanocomposite to enhance biocompatibility. *Current Nanoscience*, 9(3): 308–317.

Liu, B. and Peng, B. (2017). Modelling and optimization of process parameters for strawberry osmotic dehydration using central composite rotatable design. *Journal of Food Quality*, 2017/2593213, https://doi.org/10.1155/2017/2593213.

Oladipo, A.A., Adeleye, O.J., Oladipo, A.S., and Aleshinloye, A.O. (2017). Bioderived MgO nanopowders for BOD and COD reduction from tannery wastewater. *Journal of Water Process Engineering*, 16(1): 142–148.

Raut, A.V., Yadav, H.M., Gnanamani, A., Pushpavanam, S., and Pawar, S.H. (2016). Synthesis and characterization of chitosan-TiO_2:Cu nanocomposite and their enhanced antimicrobial activity with visible light. *Colloids and Surfaces B: Biointerfaces*, 148: 566–575.

Reddy, R.S., Ramachandra, C.T., Hiregoudar, S., Nidoni, U., Ram, J., and Kammar, M. (2014). Influence of processing conditions on functional and reconstitution properties of milk powder made from Osmanabadi goat milk by spray drying. *Small Ruminant Research*, 119(1–3): 130–137.

Sarkar, B., Chakrabarti, P.P., Vijaykumar, A., and Kale, V. (2006): Wastewater treatment in dairy industries and possibility of reuse. *Desalination*, 195(1–3): 141–152.

Thirugnanasambandham K., Sivakumar V., and Jeganathan, P.M. (2014a). Investigation on biogas production process from chicken processing industry wastewater using statistical analysis: modelling and optimization. *Journal of Renewable and Sustainable Energy*, 6(4): 043117.

Thirugnanasambandham, K. and Ganesamoorthy, R. (2019). Dual treatment of milk processing industry wastewater using electro fenton process followed by anaerobic treatment. *International Journal of Chemical Reactor Engineering*, 17(12): 20190074. https://doi.org/10.1515/ijcre-2019-0074.

Thirugnanasambandham, K. and Shine, K. (2016a). Hydrogen gas production from sago industry wastewater using electrochemical reactor: simulation and validation. *Energy Sources, Part A: Recovery, Utilization, and Environmental Effects*, 38(15): 2258–2264. https://doi.org/10.1080/15567036.2016.1174755.

Thirugnanasambandham, K. and Shine, K. (2016b). Investigation on the removal of chromium from wastewater using electrocoagulation. *International Journal of Chemical Reactor Engineering*, 16(5): 20170155, https://doi.org/10.1515/ijcre-2017-0155.

Thirugnanasambandham, K. and Sivakumar, V. (2015). Modelling and optimization of treatment of milk industry wastewater using chitosan zinc oxide nanocomposite. *Desalination and Water Treatment*, 57(40): 18630–18638. https://doi.org/10.1080/19443994.2015.1102089.

Thirugnanasambandham, K., Sivakumar, V., and Maran, J.P. (2014b). Treatment of egg processing industry effluent using chitosan as an adsorbent. *Journal of the Serbian Chemical Society*, 79(6): 743–757. https://doi.org/10.2298/JSC130201053T.

Tian, F., Liu, Y., Hu, K., and Zhao, B.Y. (2003). The depolymerization mechanism of chitosan by hydrogen peroxide. *Journal of Materials Science*, 38: 4709–4712. https://doi.org/10.1023/A:1027466716950.